Preferential solvation of lysozyme in water/ethanol mixtures

Maria Grazia Ortore, Paolo Mariani, Flavio Carsughi, Stefania Cinelli, Giuseppe Onori, José Teixeira, and Francesco Spinozzi

Citation: The Journal of Chemical Physics **135**, 245103 (2011); doi: 10.1063/1.3670419
View online: http://dx.doi.org/10.1063/1.3670419
View Table of Contents: http://scitation.aip.org/content/aip/journal/jcp/135/24?ver=pdfcov
Published by the AIP Publishing

Preferential solvation of lysozyme in water/ethanol mixtures

Maria Grazia Ortore,[1] Paolo Mariani,[1] Flavio Carsughi,[2,3] Stefania Cinelli,[4] Giuseppe Onori,[4] José Teixeira,[5] and Francesco Spinozzi[1,a)]
[1]*Department of Life and Environment Sciences, Marche Polytechnic University and CNISM, I-60131 Ancona, Italy*
[2]*Department of Agricultural Food and Environmental Sciences, Marche Polytechnic University and CNISM, I-60131 Ancona, Italy*
[3]*Jülich Center for Neutron Scattering, Forschungszentrum Jülich, D-85747 Garching, Germany*
[4]*Department of Physics, University of Perugia and CEMIN, I-06123 Perugia, Italy*
[5]*Laboratoire Léon-Brillouin, F-91191 Gif-sur-Yvette, France*

(Received 30 June 2011; accepted 29 November 2011; published online 23 December 2011)

We provide a quantitative description of the solvation properties of lysozyme in water/ethanol mixtures, which has been obtained by a simultaneous analysis of small-angle neutron scattering and differential scanning calorimetry experiments. All data sets were analyzed by an original method, which integrates the exchange equilibrium model between water and ethanol molecules at the protein surface and activity coefficients data of water/ethanol binary mixtures. As a result, the preferential binding of ethanol molecules at the protein surface was obtained for both native and thermal unfolded protein states. Excess solvation numbers reveal a critical point at ethanol molar fraction ≈0.06, corresponding to the triggering of the hydrophobic clustering of alcohol molecules detected in water/ethanol binary mixtures. © *2011 American Institute of Physics*. [doi:10.1063/1.3670419]

I. INTRODUCTION

It is widely acknowledged that the structure and dynamics of proteins are strongly influenced by interactions with water.[1,2] Measurements on the properties of water molecules associated with a protein, and particularly on their changes after conformational transitions and binding reactions, are then considered fundamental for furthering the understanding of protein hydration.

When a protein is dissolved in a mixed aqueous solution its structural and dynamic properties change as a function of the solvent composition,[3] according to a preferential solvation process, which accounts for the accumulation or reduction of the different solvent molecules at the protein surface.[4,5] It has been demonstrated, for example, that a co-solvent can act as plasticizer or stabilizer, allowing or blocking the protein to jump between the so-called conformational substates,[6] or to play as modulator for biochemical reactions.[7] Also the perspective of being able to regulate the characteristics of a protein by changing the physical and chemical environment in which it is dissolved has a relevant practical interest and noticeable consequences.

The molecular structural characterization of the protein solvation shell in a binary mixture appears very problematic due to sensitivity requirements for detecting possible small modifications of solvent composition at the protein surface. Moreover, until a few years ago, molecular dynamics simulations to study this issue were scarcely applied.[8]

On the other hand, due to a fine tuning of the scattering contrast between protein, solution, and solvation shell, we have recently showed that the small-angle neutron scattering (SANS) technique can be an optimum tool to experimentally obtain the composition of the solvation shell of a protein dissolved in binary solvents.[9–11] In particular, we demonstrated that lysozyme is preferentially hydrated when dissolved in a water/glycerol mixture, in full agreement with previous literature indications obtained at infinite protein dilution,[12] but depleted of water molecules when dissolved in a water/urea mixture,[10] again in agreement with previous data.[13] In water/glycerol mixtures, one result is specially noticeable: the excess solvation number for water (e.g., the number of water molecules around a lysozyme in solution, in excess - augmentation or depletion - to the number of water molecules contained in a volume of bulk solvent equivalent to the solvation shell volume) reported as a function of the water molar fraction in the solvent, x_w, shows a maximum at around 0.6.[9] Using differential scanning calorimetry (DSC) studies, a clear relationship between the preferential hydration and the lysozyme stability was then established,[14] as the stability of lysozyme in water/glycerol mixtures at 298 K was observed to be maximal exactly at $x_w = 0.6$.

Among other binary mixtures, monohydric alcohols/water solutions have largely been investigated. In particular, it has been clearly established that monohydric alcohols, such as methanol, ethanol and 1-propanol, destabilize the native structure of proteins, although the promotion of the α-helix conformation in unfolded proteins and peptides[15] and the stabilization of the native state for diluted solutions[16] have been also reported. In particular, ethanol has been demonstrated to modify the amyloidogenic self-assembly of insulin.[17] A large number of experimental,[18–21] theoretical,[22] and molecular dynamics studies[23–25] have been focused on the structure of the molecular clusters formed by alcohol in

a)Author to whom correspondence should be addressed. Electronic mail: f.spinozzi@univpm.it.

water. As a result, micro-heterogeneous structures of alcohol and water in binary mixtures have come to be generally accepted, and their relationship with protein stability has been highlighted. In particular, the hydrophobic clustering of ethanol molecules in a bulk aqueous solution has been experimentally investigated through detailed measurements of compressibility and frequency of C−H stretching.[18,26] Such investigations have shown that ethanol is essentially monomeric for an ethanol molar fraction in the solvent, x_e, lower than 0.06, while self-associates in the range $0.06 < x_e < 0.29$. Correlations between the microstructure of the binary solvent and the conformation of a protein therein dissolved have been demonstrated by studying the thermal denaturation of lysozyme in water/ethanol mixtures.[27] In particular, the transition enthalpy, ΔH, has been observed to depend in a complex manner on the amount of alcohol present in the solution: as ethanol concentration is increased, ΔH increases until a maximum value is reached at a mole fraction x_e^* of about 0.06. A maximum at the same mole fraction was also detected in the denaturation entropy change, ΔS.

Actually, proteins appear as sensible probes for monitoring solution properties and their complicated evolution with composition. Since existing results collectively indicate that the conformational stability of a protein is closely related to the features of the solvation shell, a complete description of the phenomenon requires taking into account the properties of the plain water/alcohol mixtures and the thermodynamic characteristics of the protein-solvent interactions.

The aim of the present study is to discuss the properties of the water/ethanol binary solution comparing SANS and DSC results on lysozyme dissolved in the mixture. Experiments were performed in parallel on similar samples, and the whole experimental data were analyzed using a global fit procedure, an approach that we have demonstrated to be very efficient for extracting tiny structural details from a wide experimental context.[9,10,14] By adopting Schellman's thermodynamic model,[28,29] based on an equilibrium exchange between water and ethanol in the bulk and in the solvation layer, we are able to estimate, for both the native and the denatured protein states, the thermodynamic equilibrium constant and related thermodynamic parameters, such as the excess solvation numbers. Since data were evaluated as a function of solvent composition, correlations with the water/ethanol binary mixture properties were also derived.

II. MATERIALS AND METHODS

A. Sample preparation

Hen egg-white lysozyme (Fluka Chemie AG) was dissolved in 0.1 M HCl/glycine water/ethanol solutions at *p*H 3.0. The lysozyme concentration was checked spectrophotometrically by using an extinction coefficient of $\varepsilon_{1\ \mathrm{cm}}^{1\%} = 26.9$ at 280 nm. Ten samples were investigated by DSC, with lysozyme concentration fixed to 20 mg/mL and ethanol molar fraction in the solvent, x_e, ranging from 0 to 0.09. Sixteen samples were studied by SANS: for each lysozyme concentration equal to 30, 60, 90, and 120 mg/mL, the values of x_e were 0, 0.03, 0.06, and 0.09. All the samples were prepared at a deuteration grade x_D equal to 0.88, according to the procedure described in the supplementary material.[30]

B. SANS experiments

SANS measurements were carried out at the Laboratoire Leon Brillouin, France, on the PAXE diffractometer. Two sample-detector distances (1 and 3 m) and 7 Å wavelength neutrons were used. The investigated exchanged wave vector modulus q ranged from 0.015 to 0.3 Å^{-1}. Samples were measured at room temperature in a 1 mm thick quartz cell. Experimental detector counts were radially averaged and corrected for sample transmission, detector inhomogeneities and scattering from buffer, and converted into macroscopic differential scattering cross section in absolute units (cm^{-1}) by direct beam measurements.[31]

C. DSC data

The DSC experiments were performed on a micro-DSC II (Setaram, France) at a scan rate of 18 Kh^{-1} with sample masses of 0.85 g. More details can be found in Ref. 27, where these data were already published.

III. THERMODYNAMIC MODEL AND DATA ANALYSIS

In brief, SANS and DSC results obtained on lysozyme dissolved in water/ethanol binary solutions were analyzed using a global fit procedure based on the mixed solvent exchange thermodynamic model. In the following, the thermodynamic model as well as the SANS and DSC data analysis will be detailed. Here, it should be noticed that few basic assumptions have been made, i.e., the lysozyme structure was considered unchanging in the range where water/ethanol ratio is varied and the unfolding process has been assumed to be cooperative and two-state at all the investigated conditions. Both assumptions are consistent with the low alcohol concentration used (less than 25% v/v) and are supported by previous results. First, in Ref. 32 the observed slight variations of lysozyme hydrodynamic radius with ethanol mole fraction between 0 and 0.08 were attributed to the effect of alcohol in modulating solvent-mediated interactions and not on protein structural changes. Second, in Ref. 33 data analysis demonstrated that the increase of the osmotic second virial coefficient in lysozyme water-ethanol solutions (with x_e ranging from 0.002 to 0.072) could be fully understood considering a Mean Force Potential for "globular proteins of constant radius." Third, the unfolding of lysozyme dissolved both in D_2O and CH_3CH_2OD/D_2O was studied by Fourier transform infrared (FTIR) absorption spectroscopy at different protein concentrations (x_e = 0.15, 30 and 120 mg/mL lysozyme concentrations).[34] The detailed description of the local and global rearrangements is compatible with a cooperative and two-state process at both the considered sample compositions.

A. Solvent exchange thermodynamic model

As shown in recent papers,[9–11,14] the number of water molecules adsorbed or released from a protein surface, as a result of modifications on the composition of the binary mixture where the protein is dissolved, can be experimentally determined both from SANS and DSC data. In particular, the mixed solvent exchange thermodynamic model formulated by Schellman,[28] which describes the protein solvation process as a thermodynamic equilibrium between solvent molecules in contact with the protein surface and in the bulk, has been demonstrated to be appropriate. By using a global fit strategy, Schellman's thermodynamic equilibrium constant appears as the main data fitting parameter, responsible for the protein shell structural, compositional and energetic features in all the set of investigated experimental conditions, which differ for protein and co-solvent concentrations.[11]

The model can be summarized in the following way. The protein surface is considered to provide m sites, which can be occupied either by water or ethanol molecules, and none of them can be unoccupied. The water and ethanol molecules in close vicinity to the protein define the "local domain" region l, which includes the solvent molecules filling the gaps between the protein bound ethanol molecules (see Fig. 4 in Ref. 9). The composition of the local domain, represented by the ethanol molar fraction $x_{e,l}$, can be different from the one of the bulk solvent, $x_{e,b}$. The ethanol-water exchange equilibrium taking place at m sites can be written as

$$e_s + w_b \rightleftharpoons e_b + w_s, \tag{1}$$

where e_s, e_b and w_s, w_b represent ethanol (e) and water (w) molecules in the bulk phase (b) and in direct contact with the protein surface (s), respectively. Note that domain s contains only water and ethanol molecules in contact with the protein surface, and therefore is a non-uniform shell around the protein. Considering the probability ϕ that m sites are occupied by water molecules, the thermodynamic exchange equilibrium constant can be translated into the equation

$$K^{\text{ex}} = \frac{\phi}{1-\phi}\frac{a_e}{a_w}, \tag{2}$$

where $a_e = \gamma_e x_{e,b}$ and $a_w = \gamma_w(1 - x_{e,b})$ are the activities of ethanol and water in the bulk domain. The corresponding activity coefficients, γ_e and γ_w, have been expressed as analytical functions of $x_{e,b}$, according to excess free energy data.[35]

Two important aspects of Eq. (2) merit to be discussed. First: since it is well known that water-ethanol mixtures differ in a relevant way from ideality, the thermodynamic availability of both water and ethanol molecules in the bulk domain is properly described by activities instead than by molar fractions.[28] Second: at our knowledge, it is not possible to design experiments by which to measure activity coefficients of molecules bound on a protein surface. Hence we can only quantitatively express the thermodynamic availability of water and ethanol molecules bound to the lysozyme surface by the simple water occupation probability ϕ of the m sites.

Equation (2) is then central in the global fit strategy adopted here. However, as DSC data contain information on lysozyme unfolding, two different thermodynamic exchange equilibria were considered in the calorimetric data analysis,[14] the first related to the solvent exchange between the bulk and the native protein surface (described by the thermodynamic exchange equilibrium constant K_N^{ex}) and the second related to the solvent exchange between the bulk and the unfolded protein surface (described by the thermodynamic exchange equilibrium constant K_U^{ex}). In this framework, the SANS experiments performed on native lysozyme enhanced the information concerning the first thermodynamic equilibrium already provided by DSC data.

B. SANS data analysis

For monodisperse and randomly oriented protein particles dissolved in a homogeneous solvent, the SANS macroscopic differential scattering cross section can be expressed as

$$\frac{d\Sigma}{d\Omega}(q) = n_p P(q) S_M(q) + B, \tag{3}$$

where n_p is the protein number density, $S_M(q)$ the effective (measured) structure factor defined by

$$S_M(q) = 1 + \frac{[F(q)]^2}{P(q)}[S(q) - 1] \tag{4}$$

in which $S(q)$ is the protein-protein structure factor, $P(q)$ the form factor, and $F(q)$ the angular average of the Fourier transformation of the scattering length density distribution of the protein.[36] Finally, B is a flat background, which accounts for incoherent scattering effects.

In the present case, the protein-protein structure factor $S(q)$ was modeled on the basis of a three-terms pair interaction potential, $u(r) = u_0(r) + u_1(r) + u_2(r)$, which includes a hard sphere potential,

$$u_0(r) = \begin{cases} \infty & r \le 2R, \\ 0 & r > 2R, \end{cases} \tag{5}$$

and two Yukawian terms, namely a repulsive coulombic screened potential, $u_1(r)$, and an attractive potential, $u_2(r)$, both of the form $u_j(r) = A_j \exp[-\kappa_j(r - 2R)]/r$.[9,11] In these expressions, R represents the effective hard-sphere protein radius. For the coulombic term, the constant A_1 depends on the net protein charge Z, on the bulk dielectric constant ε (which is a known function of the composition of the bulk, $x_{e,b}$) and on the inverse Debye length κ_1 (which is usually written as a function of Z and the ionic strength I_S due to all the microionic species in solution, as in Eq. (11) in Ref. 37). Concerning the attractive Yukawian term, the pre-exponential constant is written as $A_2 = -2RJ$, where J is the so-called potential at protein-protein contact, whereas the constant κ_2 is simply written as the inverse of the decay length d.

The calculation of $S(q)$ from the potential $u(r)$ requires the solution of the Ornstein-Zernike (OZ) equation under a proper choice of a closure. A very efficient closure method for a two-Yukawa potential, based on a numerical solution of the mean-spherical approximation (MSA), originally developed by Liu, Chen, and Chen[38] was successfully applied

in the analysis of SANS data of proteins in a wide range of concentrations.[38–41] These studies have shown that the subtle balance between attractive and repulsive potentials leads to a transition from a monomer fluid to a cluster fluid at increasing protein concentration. In particular, the appearance of a peak in the structure factor whose position does not scale with the $n_p^{1/3}$, as expected for a fluid of not interacting monomers, suggests an intermediate range order, as it has been recently discussed in many experimental and theoretical works.[41–43] In this study, the strong repulsion regime due to the acidic conditions of our samples led us to choice the simple and analytical Random-Phase Approximation (RPA), where $S(q)$ is expressed as a perturbation of the well-known hard-sphere structure factor $S_0(q)$ according to PY closure[44,45] (see supplemental material[30] for details).

$F(q)$ and $P(q)$ were evaluated from the lysozyme atomic coordinates reported in the Protein Data Bank (PDB entry `6lyz` (Ref. 46)) and taking into account the composition of the protein solvation layer. The SASMOL approach,[47,48] which locates the sites of the water molecules belonging to the different protein hydration shells and describes them as Gaussian spheres, was used. According to the SASMOL method, the number of sites belonging to the lysozyme first hydration shell (corresponding to the m sites of the s-domain) was 385, whereas in the second shell $m' = 470$ sites were found. Since the molecular volume of ethanol is larger than that of water, the local domain l has been considered to include both the first hydration shell, of which a fraction ϕ is occupied by water molecules, and the second hydration shell of the protein, whose ethanol composition corresponds to $x_{e,b}$. The calculation of the values of ϕ and $x_{e,b}$, which for a fixed thermodynamic exchange constant are functions of the nominal sample composition (expressed by n_p and x_e), has been performed by numerically solving the system constituted by the Eq. (2) (using the dependency of γ_e and γ_w on $x_{e,b}$) and the mass balance of the system. The local domain composition, $x_{e,l}$, was then calculated by averaging the compositions of the sites in the first and in the second hydration shells. Therefore, the form factor depends on solvent composition (ethanol concentration and deuteration grade) and on the thermodynamic parameters fixing the compositional relationships among the different domains[9] (see the supplementary material[30] for the resulting equations).

C. DSC data analysis

DSC analysis was based on the two-state transition model described by Schwarz and Kirchhoff[49] updated under the quantitative advisement of the 4 components of the system: folded and unfolded lysozyme, water and ethanol. On the basis of previous reports, the unfolding process has been assumed to be cooperative and two-state at all the investigated conditions.[34] Thermodynamic exchange constants, K_N^{ex} and K_U^{ex}, and the number of exchange sites on the unfolded protein (m_U) had to be determined.

DSC thermograms, reporting the temperature dependence of the heat capacity C_p of the protein dissolved in the water/ethanol mixtures, were calculated following the Schellman's exchange model as reported by Spinozzi *et al.*[14]

$$C_p = C_{pN} + \frac{n_{p,U}}{n_p}\left[\Delta C_p + \frac{(\Delta H)^2}{(\exp(-\Delta G/k_BT)+1)k_BT^2}\right], \tag{6}$$

where $n_{p,U}$ is the number density of unfolded lysozyme, $\Delta C_p = C_{pU} - C_{pN}$, ΔH and ΔG are the differencies of heat capacity, enthalpy, and free energy for the transition between native and unfolded protein, each conformation having a different composition of the solvation shell, as represented by the following expression:

$$\begin{aligned} N w_{m_N\phi_N} e_{m_N(1-\phi_N)} + (m_U\phi_U - m_N\phi_N)w \\ +[m_U(1-\phi_U) - m_N(1-\phi_N)]e \\ \rightleftharpoons U w_{m_U\phi_U} e_{m_U(1-\phi_U)}. \end{aligned} \tag{7}$$

All terms in Eq. (6) are complex functions of composition (x_e and n_p) and temperature.[14] It has to be stressed that the whole unfolding equilibrium described by Eq. (7) can be decomposed in three elementary parts: (i) an unfolding equilibrium of lysozyme in water, (ii) m_N water/ethanol exchange equilibria at the surface of the protein in the native conformation, (iii) m_U water/ethanol exchange equilibria at the surface of the unfolded protein. Because any water/ethanol exchange over folded and unfolded protein modifies the composition of the bulk solvent ($x_{e,b}$), the model takes into account the contribution of excess enthalpy, excess heat capacity and excess volume of water/ethanol mixtures, which are calculated as analytical functions of $x_{e,b}$ by means of published phenomenological expressions.[50–52] Hence, all thermodynamic functions were written as proper combinations of the thermodynamic functions of each of the three elementary transitions.

D. Global fit analysis

A global fitting procedure was used to provide a unique interpretation of the whole set of experimental data. All the 26 experimental curves (10 DSC thermograms and 16 SANS curves) were analyzed together, and three different classes of fitting parameters were considered. The first class includes common parameters, which are independent of the type of experiment and of the experimental condition, such us K_N^{ex}; the second class includes common parameters which are pertinent only to SANS or DSC, but are still independent on the experimental condition; the third class includes parameters which depend on sample composition, deuteration grade, and type of experiment and should be fitted independently for each curve. Further details concerning the fitting parameters can be found in the supplementary material.[30]

IV. RESULTS AND DISCUSSION

SANS and DSC fitting results are superimposed to experimental data in Figs. 1 and 2: the good quality of the fitting procedure, also indicated by the rather low value of 1.23 for the global reduced χ^2, can be easily appreciated. The common parameters resulting from the global fittings are reported in Table I.

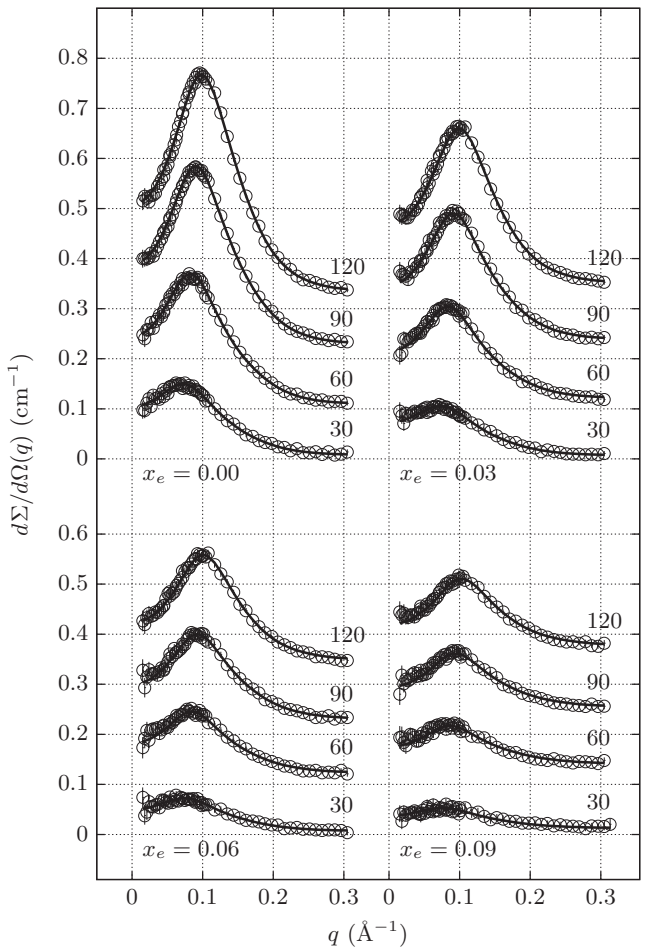

FIG. 1. SANS curves of lysozyme in water/ethanol mixtures at different compositions, as shown by the x_e values reported in the bottom of each column and by the protein concentration reported on the right of each curve in mg/mL unit. All the samples are at a deuteration grade $x_D = 0.88$. Circles correspond to experimental data, solid lines are the best fits obtained by the global fit analysis. Curve are scaled by a factor 0.1 cm^{-1} for clarity.

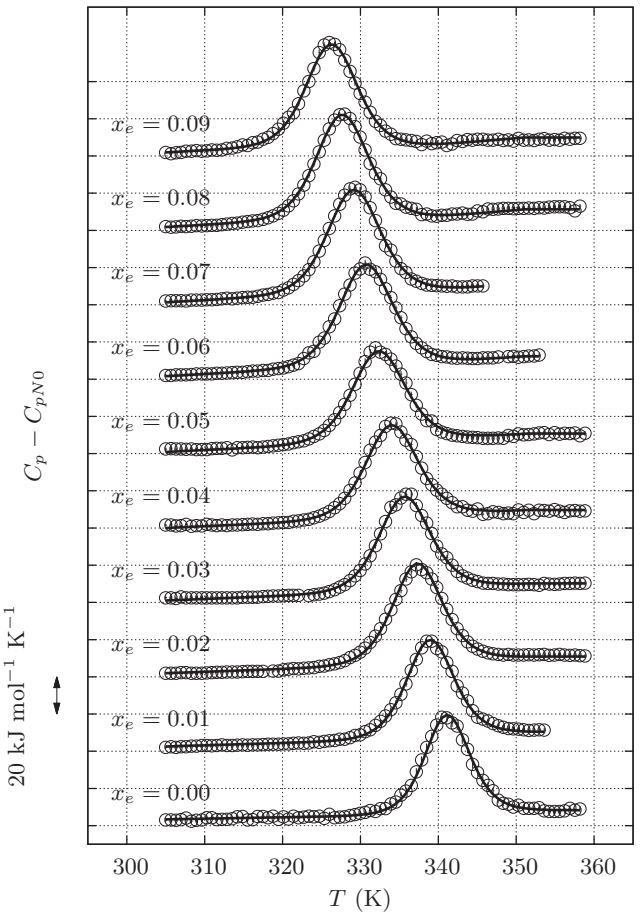

FIG. 2. Experimental DSC thermal scans of lysozyme in water/ethanol mixtures at different compositions, as shown by the indicated x_e values. Circles correspond to the experimental data. Solid lines represent the profiles obtained by the global fit analysis. Curves are scaled by 40 kJ mol^{-1}K^{-1} for clarity.

Before analyzing the thermodynamic exchange constants, which dictate the composition of the local domain, few comments on the fitted structural parameters are mandatory. The protein effective charge Z resulted nearly independent on protein and ethanol concentration: its average value resulted $\langle Z \rangle = 16.0 \pm 0.3$ e, which roughly corresponds to the number of charges carried by lysozyme at *p*H 3 according to its aminoacid composition.[53] Considering the attractive term, the decay length d was found to be almost constant with the ethanol mole fraction, with an average value $\langle d \rangle = 3.0 \pm 0.4$ Å, whereas the depth J was observed to slightly decrease (~3%, from 12.2 ± 0.4 kJ mol^{-1} at $x_e = 0.00$ to 10.9 ± 0.4 kJ mol^{-1} at $x_e = 0.09$). We notice that the values of J result to be larger compared to those obtained in similar experimental conditions by MSA (Refs. 40 and 41) and HNC closure.[54] This difference may be attributed to the use in our analysis of structure factors expressed in the RPA approximation which, as it is well known, tends to overestimate the attractive component of the potential. However, the RPA approximation does not influence the observed trend of the depth of the attractive potential versus ethanol molar content in solution.

From one hand, the decrease of the depth J is rather interesting, as it confirms previous observations suggesting that the increase of lysozyme repulsive forces in the presence of ethanol (detected as an increase of the osmotic second virial coefficient induced by addition of ethanol on aqueous lysozyme solution) is mainly determined by reduced attractive hydrophobic interactions and not by changes in the coulombic repulsion.[33]

On the other hand, the observation of a nearly constant Z disagrees with recent SANS data analysis on lysozyme aqueous solution, which showed a net charge increase from ca. 8 to 10 e when protein concentration changes from 5 to 22.5%.[41] However, in that case the *p*D of the protein solutions was barely controlled (the *p*D value was 6.8 at 5% and 4.5 at 22.5%[41]), and the different used closure of the OZ equation to obtain the structure factor may account for the discrepancy, too. Indeed, some discordances between the attraction strengths calculated by using MSA and Hypernetted Chain closures were even underlined by the authors.[41] As the structure factors are not expected to change with the choice of the closure (and then can be directly compared), effective structure factors at different lysozyme and ethanol concentrations have been extracted from SANS curves by dividing the experimental macroscopic differential scattering cross section

TABLE I. First, second, and third class global fit parameters of SANS and DSC data (symbols as in the text and in the supplementary material[30]). Errors in fitting parameters were established by iteratively moving all the SANS and DSC curve points within their experimental error, by then repeating the minimization process and by calculating the average and the standard deviation of each fitting parameter after a number of iterations equal to 20.

First class parameters			
	K_N^{ex}		
	2.67 ± 0.04		
Second class parameters and average third class parameters, SANS			
$\langle Z \rangle$	$\langle d \rangle$	$v_{w,s}$	
(e)	(Å)	(Å^3)	
16.0 ± 0.3	3.0 ± 0.4	29.3 ± 0.1	
Third class parameters, SANS			
$\langle J \rangle_{x_e=0.00}$	$\langle J \rangle_{x_e=0.03}$	$\langle J \rangle_{x_e=0.06}$	$\langle J \rangle_{x_e=0.09}$
(kJ mol^{-1})	(kJ mol^{-1})	(kJ mol^{-1})	(kJ mol^{-1})
12.2 ± 0.4	11.8 ± 0.3	11.4 ± 0.3	10.9 ± 0.4
Second class parameters, DSC			
K_U^{ex}		m_U	
2.54 ± 0.02		418 ± 2	
ΔH_{w0}		ΔG_{w0}	
(kJ mol^{-1})		(kJ mol^{-1})	
270 ± 10		48 ± 1	
C_{pwU0}	C_{pwN1}	C_{pwU1}	
(kJ mol^{-1} K^{-1})	(J mol^{-1}K^{-2})	(J mol^{-1}K^{-2})	
7.6 ± 0.6	130 ± 20	32 ± 7	
$\Delta H_{N0}^{\mathrm{ex}}$	$\Delta H_{U0}^{\mathrm{ex}}$	$\Delta C_{pN0}^{\mathrm{ex}}$	$\Delta C_{pU0}^{\mathrm{ex}}$
(kJ mol^{-1})	(kJ mol^{-1})	(J mol^{-1} K^{-1})	(J mol^{-1} K^{-1})
6.8 ± 0.5	-0.2 ± 0.1	12 ± 4	220 ± 20

by the fitted form factor of the solvated protein. Results are reported in Fig. 3. At one side, it can be observed that the form factors strongly depend on x_e (e.g., on the composition of the solvation layer), while do not change with protein concentrations, as expected. On the other side, the structure factors appear almost independent on ethanol addition but dependent on protein concentration, confirming that the interprotein potential is dominated by a strong repulsive regime (probably due to the large number of charges on lysozyme at this *p*H) and suggesting that the eventual formation of small equilibrium clusters[43,55] is prevented. Moreover, $S_M(q)$ shows only one peak, at about 0.1 Å^{-1}, while the second peak, observed by Liu *et al.*[41] at about 0.23 Å^{-1} and prominent at high lysozyme concentration, is absent (or only barely visible). The pronounced shift of the first maximum toward higher q with increasing concentration, although does not follow a $n_p^{1/3}$ behavior (see the inset in the left panel of Fig. 3), appears in contrast with the attribution of this peak to cluster-cluster correlations[55] and is clearly more compatible with a system dominated by largely repulsive individual lysozyme molecules in solution, as also observed by Shukla *et al.*[42]

The main quantitative results of the present analysis are however the thermodynamic exchange constants K_N^{ex} and K_U^{ex}. Figure 4 reports the ethanol molar fraction in the local domain, $x_{e,l}$, calculated on the basis of the fitted thermodynamic exchange constants, as a function of ethanol nominal content of the solution, x_e. Considering that the thin dashed line represents the effective constant $K^{\mathrm{ex}}\gamma_w/\gamma_e = 1$, it appears

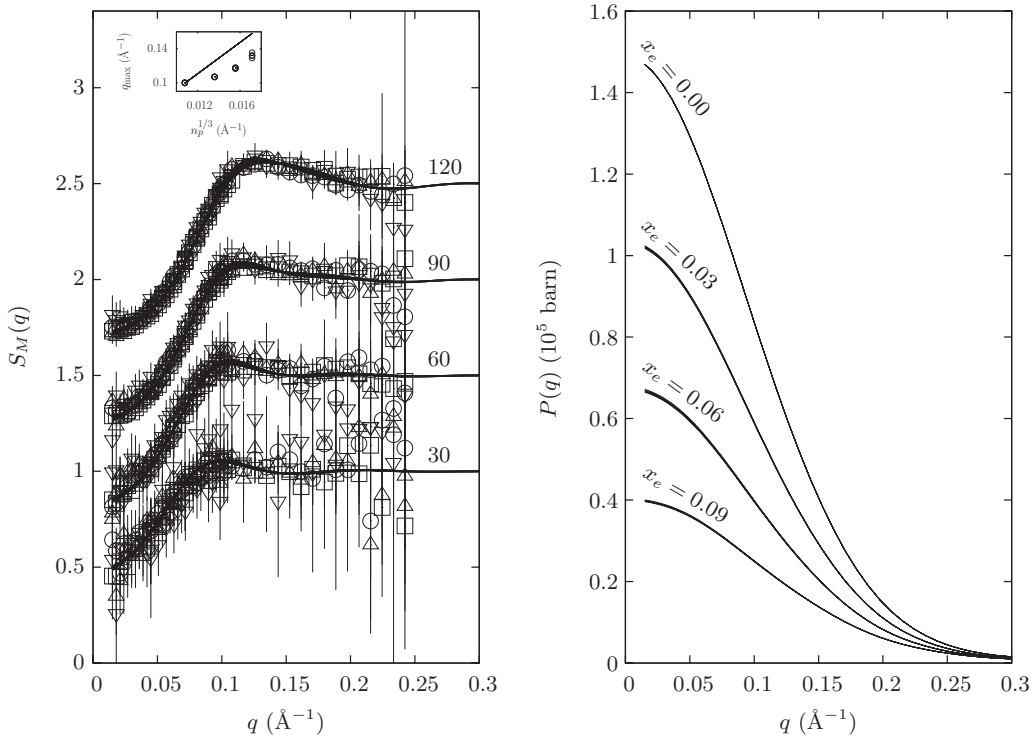

FIG. 3. Left panel. Effective structure factors calculated by $[\frac{d\Sigma}{d\Omega}(q) - B]/P(q)$. Solid lines are the effective structure factors obtained by the global-fit analysis. The four groups of curves, scaled by a factor 0.5, refer to the different protein concentration, as reported on the right in mg/mL unit. Symbols represent ethanol molar fractions: ◯, $x_e = 0.00$; □ , $x_e = 0.03$; △, $x_e = 0.06$; ▽, $x_e = 0.09$. The inset reports the first maximum positions $q_{\max}$ of $S_M(q)$ as a function of the cubic root of lysozyme number density, $n_p^{1/3}$. The solid straight line shows the behavior $q_{\max} \sim n_p^{1/3}$ expected for purely repulsive charged monomers. Right panel. Form factors obtained by the fit of SANS curves, reported in absolute units (barn). Variations of $P(q)$ with protein concentration, at fixed x_e, are within the width of the curves.

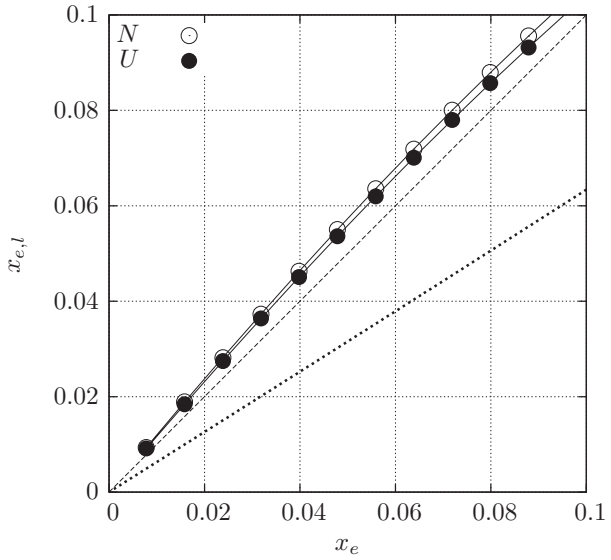

FIG. 4. Ethanol molar fraction in the local domain as a function of ethanol nominal content. The thin dashed line represents the effective constant $K^{ex}\gamma_w/\gamma_e = 1$. Continuous lines with points result from the global fit of native (open circles) and unfolded (close circles) lysozyme dissolved in water/ethanol mixtures. The dotted line shows the local domain vs. the nominal glycerol molar fraction for native lysozyme in water/glycerol mixtures, as obtained by Sinibaldi *et al.*[9]

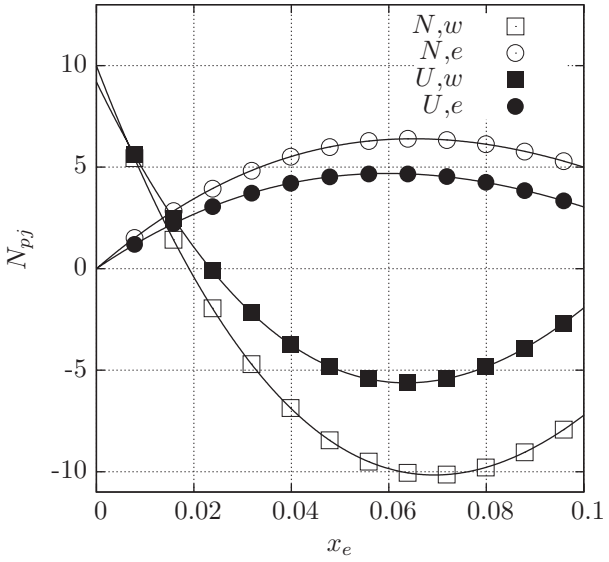

FIG. 5. Number of excess molecules of the species *j* in the lysozyme solvation layer as a function of ethanol nominal content. Circles refers to ethanol and squares to water. Empty and filled symbols refer to the native and to the unfolded protein, respectively.

evident that in water/ethanol mixtures there is a release of water molecules from the lysozyme surface, which in opposition enriches in alcohol. This is a very interesting result, as according to our knowledge no quantitative description of the protein solvation shell in a water/ethanol mixture has been previously reported, even though in a SANS study of ribonuclease in water/glycerol and water/ethanol mixtures, Lehmann and Zaccai already suggested that "For ethanol it is even possible that there might be some preferential binding."[56] Here, however, the quantitative description of the lysozyme solvation shell also concerns the unfolded protein: this is a very interesting issue, which can be related to the contribution of co-solvents with respect to protein unfolding "in vivo," as recently evidenced with force spectroscopy measurements.[5]

Concerning the results, it appears that K_N^{ex} is slightly larger than K_U^{ex} (2.67 ± 0.04 and 2.54 ± 0.02, respectively, while the number of sites appears to increase from $m_N = 385$, estimated for the native state, to $m_U = 418 \pm 2$, observed for the unfolded lysozyme. The increase in the number of sites is in full agreement with the presence of a higher protein surface exposed to the solvent upon thermal unfolding (even if the small difference is consistent with the occurrence of a molten globule conformation[34]), while the meaning of the thermodynamic exchange constant values merits to be further discussed.

The first parameter that can be derived is the so-called excess solvation number, N_{pj}, which represents the difference between the number of *j*-molecules ($j = w, e$) occupying the volume of the protein shell and those occurring in a similar volume in the bulk solvent. N_{pj} values, calculated by using Eq. (16) of Sinibaldi *et al.*,[9] are reported as a function of solvent composition in Fig. 5 (note that the excess solvation number for water is different from zero even in pure water because of the higher density of water molecules in the local domain). Two points could be underlined: at one side, the composition of ethanol in the local domain is higher than that in the bulk, in close resemblance of the behavior observed in the case of BSA[13,57] and of lysozyme[10] dissolved in urea aqueous solutions. Noticeable, in both solvents the protein structure stability is strongly reduced. At the other side, the excess solvation numbers for native lysozyme show a critical point exactly at the same concentration in which a transition in water/ethanol mixtures has been detected. In fact, both the apparent ethanol molar compressibility and the frequency of the C−H vibrations vary as a function of solvent composition starting from about $x_e^* \simeq 0.05$.[27] This finding confirms the idea that a protein can be a probe to evidence binary mixtures properties. Also interesting is the fact that a criticality in the melting temperature of Yeast Frataxin cold denaturation in water/ethanol mixtures was observed at a similar ethanol concentration,[58] while some of us recently determined that the same critical ethanol concentration triggers DNA condensation in water/ethanol mixture.[59] The criticality in the excess solvation numbers can hence be associated with the appearance of a sort of hydrophobic clustering of alcohol molecules.[26] While in the water rich region, a simple thermodynamic equilibrium between water and ethanol molecules in the bulk and in the solvation shell exists, it is possible that ethanol clustering affects this equilibrium beyond x_e^*. Consequently, ethanol can be found in solution as free molecules in the bulk, molecules bound on the protein surface or molecules forming clusters in the bulk. This picture is however implicitly taken into consideration in our model, which implements activity coefficients: for this region, a unique thermodynamic exchange constant succeeds in analyzing all the investigated experimental data.

Figure 5 also shows that the protein in the native state releases more water than the protein in the unfolded state. This finding could be considered counterintuitive, as it is com-

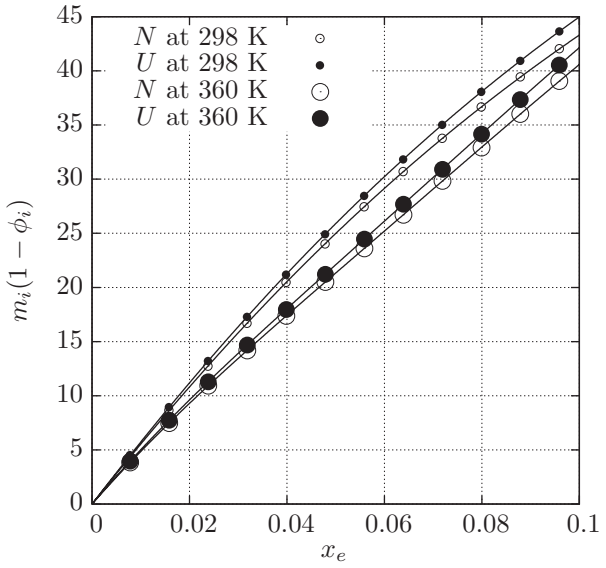

FIG. 6. Number of ethanol molecules bound to the surface of lysozyme in the native, $m_N(1-\phi_N)$, and in the unfolded, $m_U(1-\phi_U)$, state, for the two reported temperatures, as a function of the ethanol nominal content.

monly assumed that unfolded states expose more hydrophobic residues to the solvent than the native state, so that higher affinity to ethanol (that is more hydrophobic than water) for the unfolded protein could be expected. However, such a result needs to be read together with the number of protein sites upon unfolding, which increases from 385 to 418. Indeed, Fig. 6 shows the total number of ethanol molecules bound to the surface of native and unfolded lysozyme calculated as a function of x_e at two different temperatures (298 K and 360 K). As expected, more ethanol interacts with the lysozyme in the unfolded state than in the native state.

Even if the small decreasing in the ethanol preferentially affinity over the binding site from the folded to the thermally unfolded state, followed by a small increase of the total number of sites, has to be regarded within the model approximations, it should be observed that protein folded and unfolded forms can experience different solvation mechanisms, due for example to a competition engaged by alcohol molecules in the interaction with the apolar groups of the protein[58] or according to the remarkable observation that hydrophobicity manifests itself differently on large and small length scales.[60] Hence the difference between K_U^{ex} and K_N^{ex} cannot easily be explained without a deeper knowledge of the thermally exposed sites.

It is worth noting that the data analysis strategy exploited in our study is able to determine not only whether there is a preferential hydration or not, but it additionally provides values for the excesses or deficits of water and co-solvent molecules in the vicinity of lysozyme. Note that the excess or deficit of solvent molecules close to the protein surface represents the behavior of the whole protein molecule, but not for particular functional groups of the protein. In fact it is surely possible that ethanol is in excess around the whole lysozyme but in deficit in the vicinity of certain functional groups.[61] However the molecular approach of this study cannot be denied by the absence of details on specific functional binding of ethanol on protein surface.

Protein solvation issue is intimately tied to protein structural integrity and flexibility, hence to its dynamics and function. For the first time, this study provides a simultaneous analysis of SANS and DSC experimental data in order to obtain a more quantitative knowledge of the thermodynamic processes at the basis of protein solvation equilibria in binary mixtures.

[1] M. C. Bellissent-Funel, *Hydration Processes in Biology* (IOS, Amsterdam, 1999).
[2] T. M. Raschke, Curr. Opin. Struct. Biol. **16**, 152 (2006).
[3] C. M. Othon, O. Kwon, M. M. Lin, and A. H. Zewail, Proc. Natl. Acad. Sci. U.S.A. **106**, 12593 (2009).
[4] J. A. Schellman, Q. Rev. Biophys. **38**, 351 (2005).
[5] L. Dougan, G. Feng, H. Lu, and J. M. Fernandez, Proc. Natl. Acad. Sci. U.S.A. **105**, 3185 (2008).
[6] H. Fraunfelder, S. G. Sligar, and P. G. Wolynes, Science **254**, 1598 (1991).
[7] S. N. Timasheff, Proc. Natl. Acad. Sci. U.S.A. **99**, 9721 (2002).
[8] Q. Zou, B. J. Bennion, V. Daggett, and K. P. Murphy, J. Am. Chem. Soc. **124**, 1192 (2002).
[9] R. Sinibaldi, M. G. Ortore, F. Spinozzi, F. Carsughi, H. Frielinghaus, S. Cinelli, G. Onori, and P. Mariani, J. Chem. Phys. **126**, 235101 (2007).
[10] M. G. Ortore, R. Sinibaldi, F. Spinozzi, F. Carsughi, D. Clemens, A. Bonincontro, and P. Mariani, J. Phys. Chem. B **112**, 12881 (2008).
[11] M. G. Ortore, R. Sinibaldi, F. Spinozzi, A. Carbini, F. Carsughi, and P. Mariani, J. Phys.: Conf. Ser. **177**, 012007 (2009).
[12] K. Gekko and S. N. Timasheff, Biochem. **20**, 4667 (1981).
[13] S. N. Timasheff and G. Xie, Biophys. Chem. **105**, 421 (2003).
[14] F. Spinozzi, M. G. Ortore, R. Sinibaldi, P. Mariani, A. Esposito, S. Cinelli, and G. Onori, J. Chem. Phys. **129**, 35101 (2008).
[15] R. M. Parodi, E. Bianchi, and A. Ciferri, J. Biol. Chem. **248**, 4047 (1973).
[16] T. S. Banipal and G. Singh, Thermochim. Acta **412**, 63 (2004).
[17] W. Dzwolak, S. Grudzielanek, V. Smirnovas, R. Ravindra, C. Nicolini, R. Jansen, A. Loksztejn, S. Porowski, and R. Winter, Biochemistry **44**, 8948 (2005).
[18] G. Onori and A. Santucci, J. Mol. Liq. **69**, 161 (1996).
[19] A. Wakisaka and T. Ohki, Faraday Discuss. **129**, 231 (2005).
[20] A. K. Soper, L. Dougan, J. Crain, and J. L. Finney, J. Phys. Chem. **110**, 3472 (2006).
[21] J. H. Guo, Y. Luo, A. Augustsson, S. Kashtanov, J. E. Rubensson, D. K. Shuh, H. Ågren, and J. Nordgren, Phys. Rev. Lett. **91**, 157401 (2003).
[22] S. J. Suresh and V. M. Naik, J. Chem. Phys. **116**, 4212 (2002).
[23] S. K. Allison, J. P. Fox, J. P. Hargreaves, and S. P. Bates, Phys. Rev. B **71**, 024201 (2005).
[24] C. Zhang and X. Yang, Fluid Phase Equilib. **231**, 1 (2005).
[25] A. B. Roney, B. Space, E. W. Castner, R. L. Napoleon, and P. B. Moore, J. Phys. Chem. B **108**, 7389 (2004).
[26] M. D'Angelo, G. Onori, and A. Santucci, J. Chem. Phys. **100**, 3107 (1994).
[27] S. Cinelli, G. Onori, and A. Santucci, J. Phys. Chem. B **101**, 8029 (1997).
[28] J. A. Schellman, Biopolymers **34**, 1015 (1994).
[29] J. A. Schellmann, Biophys. J. **85**, 108 (2003).
[30] See supplementary material at http://dx.doi.org/10.1063/1.3670419 for deuteration grade determination, structure factor under RPA, compositions and scattering length densities of the bulk and the local domains, and list of the classified global fit parameters.
[31] J. Teixeira, in *Structure and Dynamics of Strongly Interacting Colloids and Supramolecular Aggregates in Solution*, edited by S.-H. Chen, J. S. Huang, and P. Tartaglia (Springer, New York, 1992), pp. 635–658.
[32] V. Calandrini, G. Onori, and A. Santucci, J. Mol. Struct. **565**, 183 (2001).
[33] W. Liu, D. Bratko, J. M. Prausnitz, and H. W. Blanch, Biophys. Chemistry **107**, 289 (2004).
[34] P. Sassi, G. Onori, A. Giugliarelli, M. Paolantoni, S. Cinelli, and A. Morresi, J. Mol. Liq. **159**, 112 (2011).
[35] R. S. Hansen and F. A. Miller, J. Phys. Chem. **58**, 193 (1954).
[36] S. H. Chen, Annu. Rev. Phys. Chem. **37**, 351 (1986).
[37] F. Spinozzi, D. Gazzillo, A. Giacometti, P. Mariani, and F. Carsughi, Biophys. J. **82**, 2165 (2002).
[38] Y. Liu, W. R. Chen, and S. H. Chen, J. Chem. Phys. **122**, 044507 (2005).
[39] M. Broccio, D. Costa, Y. Liu, and S. H. Chen, J. Chem. Phys. **124**, 084501 (2006).

[40]S. H. Chen, M. Broccio, Y. Liu, E. Fratini, and P. Baglioni, J. Appl. Cryst. **40**, s321 (2007).
[41]Y. Liu, L. Porcar, J. Chen, W. R. Chen, P. Falus, A. Faraone, E. Fratini, and K. H. P. Baglioni, J. Phys. Chem. B **115**, 7238 (2011).
[42]A. Shukla, E. Mylonas, E. D. Cola, S. Finet, P. Timmins, T. Narayanan, and D. I. Svergun, Proc. Natl. Acad. Sci. U.S.A **105**, 5075 (2008).
[43]F. Cardinaux, E. Zaccarelli, A. Stradner, S. Bucciarelli, B. Farago, S. U. Egelhaaf, F. Sciortino, and P. Schurtenberger, J. Phys. Chem. B **115**, 7227 (2011).
[44]M. S. Wertheim, Phys. Rev. Lett. **10**, 321 (1963).
[45]J. P. Hansen and I. R. McDonald, *Theory of Simple Liquids* (Academic, London, 1976).
[46]R. Diamond, J. Mol. Biol. **82**, 371 (1974).
[47]M. G. Ortore, F. Spinozzi, P. Mariani, A. Paciaroni, L. Barbosa, H. Amenitsch, M. Steinhart, J. Ollivier, and D. Russo, J. R. Soc. Interface **6**, S619 (2009).
[48]F. Spinozzi, GENFIT, 2009, http://www.isf.univpm.it/biophysics/software.htm.
[49]F. P. Schwarz and W. H. Kirchhoff, Thermochim. Acta **128**, 267 (1988).
[50]J. A. Boyne and A. G. Williamson, J. Chem. Eng. Data **12**, 318 (1967).
[51]J. P. E. Golier and E. Wilhelm, Fluid Phase Equilib. **6**, 283 (1981).
[52]B. Gonzalez, N. Calvar, E. Gomez, and A. Dominguez, J. Chem. Thermodynamics **39**, 1578 (2007).
[53]L. I. G. Toldo, Jambw chapter 3.1.6, (1997).
[54]A. Tardieu, A. L. Verge, M. Malfois, F. Bonnete, S. Finet, M. Reis-Kautt, and L. Belloni, J. Crystal Growth **196**, 193 (1999).
[55]A. Stradner, H. Sedgwick, F. Cardinaux, W. C. K. Poon, S. U. Egelhaaf, and P. Schurtenberger, Nature (London) **432**, 492 (2004).
[56]M. S. Lehmann and G. Zaccai, Biochemistry **23**, 1939 (1984).
[57]R. Sinibaldi, M. G. Ortore, F. Spinozzi, S. de Souza Funari, J. Teixeira, and P. Mariani, Eur. Biophys. J. **37**, 673 (2008).
[58]S. R. Martin, V. Esposito, P. D. L. Rios, A. Pastore, and P. A. Temussi, J. Am. Chem. Soc. **130**, 9963 (2008).
[59]S. Marchetti, S. Cinelli, and G. Onori, Chem. Phys. Lett. **493**, 158 (2010).
[60]B. J. Berne, J. D. Weeks, and R. Zhou, Annu. Rev. Phys. Chem. **60**, 85 (2009).
[61]I. L. Shulgin and E. Ruckenstein, J. Chem. Phys. **123**, 054909 (2005).